

Tetrahydro-1,8-naphthyridinol Analogues of α -Tocopherol as Antioxidants in Lipid Membranes and Low-Density Lipoproteins

Tae-gyu Nam,[†] Christopher L. Rector,[†] Hye-young Kim,[†] Andreas F.-P. Sonnen,[‡] Roland Meyer,[‡] Werner M. Nau,[‡] Jeffrey Atkinson,[§] Julia Rintoul,[§] Derek A. Pratt,^{*,#} and Ned A. Porter^{*,†}

Contribution from the Center in Molecular Toxicology and Vanderbilt Institute of Chemical Biology, Department of Chemistry, Vanderbilt University, Nashville, Tennessee 37235, School of Engineering and Science, Jacobs University Bremen, Campus Ring 1, D-28759 Bremen, Germany, Department of Chemistry and Centre for Biotechnology, Brock University, St. Catharines, Ontario L2S 3A1, Canada, and Department of Chemistry, Queen's University, Kingston, Ontario K7L 3N6, Canada

Received April 4, 2007; E-mail: pratt@chem.queensu.ca; n.porter@vanderbilt.edu

Abstract: Recently we demonstrated that the C(7)-unsubstituted tetrahydro-1,8-naphthyridin-3-ol has more than an order of magnitude better peroxy radical trapping activity than α -tocopherol (α -TOH) in inhibited autoxidations in benzene. In order to prepare analogues more structurally related to α -TOH for further studies *in vitro* and *in vivo*, we developed synthetic approaches to C(7)-monoalkyl and C(7)-dialkyl analogues using a sequence involving (1) AgNO₃-mediated hydroxymethyl radical addition to 1,8-naphthyridine, (2) regioselective alkyllithium addition by cyclic chelation in a nonpolar solvent, (3) iodination of the naphthyridine at C(3), and (4) CuI-mediated benzyloxylation of the aryl iodide followed by catalytic hydrogenolysis. An α -TOH isostere was prepared by a Wittig coupling of a C₁₆ side chain identical to that of α -TOH to the naphthyridinols. The C(7)-mono- and dialkyl analogues exhibited more than an order of magnitude higher antioxidant activity ($k_{inh} = (5.3\text{--}6.1) \times 10^7 \text{ M}^{-1} \text{ s}^{-1}$) than α -TOH ($k_{inh} = 0.35 \times 10^7 \text{ M}^{-1} \text{ s}^{-1}$) in benzene, as determined by a newly developed peroxy radical clock. In addition to the strong antioxidant activity in benzene, the closest α -TOH analogue (naphthyridinol-based tocopherol, N-TOH) showed excellent inhibition of the oxidation of cholesteryl esters in human low-density lipoprotein and spared endogenous α -TOH in these experiments. Lateral diffusion of N-TOH in 1-palmitoyl-2-oleoyl-*sn*-glycero-3-phosphocholine liposomes was comparable to that of α -TOH, suggesting that it will have good antioxidant characteristics in both membranes and lipoproteins. Furthermore, a binding assay using a fluorescent tocopherol analogue showed that N-TOH binds to recombinant human tocopherol transfer protein better than α -TOH itself, suggesting that distribution of unnatural antioxidants such as N-TOH *in vivo* is possible.

Introduction

Lipid peroxidation is a free radical chain reaction (eqs 1–4)¹ implicated in various pathologies such as cancer,² cardiovascular disease,^{3,4} and neurodegeneration.⁵ α -Tocopherol (α -TOH), nature's best lipid-soluble chain-breaking antioxidant, efficiently inhibits lipid peroxidation by scavenging chain-carrying lipid peroxy radicals, LOO[•], as shown in eqs 5 and 6.⁶ The antioxidant activity of α -TOH is attributed to its low O–H bond

dissociation enthalpy (BDE), and much effort has been devoted to the development of antioxidants with weaker O–H BDEs and a consequent better activity than α -TOH.



We recently reported^{7,8} that 6-amino-3-pyridinols are efficient chain-breaking antioxidants. For example, the bicyclic 6-amino-

[†] Vanderbilt University.

[‡] Jacobs University Bremen.

[§] Brock University.

[#] Queen's University.

(1) Porter, N. A. *Acc. Chem. Res.* **1986**, *19*, 262.

(2) Marnett, L. J. *Carcinogenesis* **2000**, *21*, 361–370.

(3) Steinberg, D.; Parthasarathy, S.; Carew, T. E.; Khoo, J. C.; Witztum, J. L. *New Engl. J. Med.* **1989**, *321*, 1196–1197.

(4) Glass, C. K.; Witztum, J. L. *Cell* **2001**, *104*, 503–516.

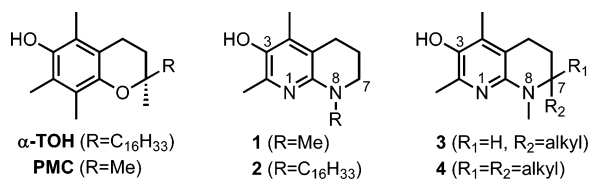
(5) Zagol-Ikapitte, I.; Masterson, T. S.; Amarnath, V.; Montine, T. J.; Andreasson, K. I.; Boutaud, O.; Oates, J. A. *J. Neurochem.* **2005**, *94*, 1140–1145.

(6) Burton, G. W.; Ingold, K. U. *J. Am. Chem. Soc.* **1981**, *103*, 6472–6477.

(7) Wijnmans, M.; Pratt, D. A.; Valgimigli, L.; DiLabio, G. A.; Pedulli, G. F.; Porter, N. A. *Angew. Chem., Int. Ed.* **2003**, *42*, 4370–4373.

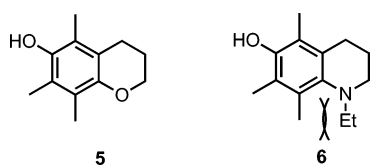
(8) Wijnmans, M.; Pratt, D. A.; Brinkhorst, J.; Serwa, R.; Valgimigli, L.; Pedulli, G. F.; Porter, N. A. *J. Org. Chem.* **2004**, *69*, 9215–9223.

3-pyridinol (or tetrahydro-1,8-naphthyridinol) **1** displayed a 25-fold larger inhibition rate constant for reactions with chain-propagating peroxy radicals ($k_{\text{inh}} = k_5 = 8.8 \times 10^7 \text{ M}^{-1} \text{ s}^{-1}$)⁷ than did α -TOH ($k_{\text{inh}} = 3.5 \times 10^6 \text{ M}^{-1} \text{ s}^{-1}$) in benzene. Monocyclic 6-amino-3-pyridinols showed lower activity than **1** yet were still several times better than α -TOH. Air stability, which limits the efficacy of electron-rich antioxidants, is significantly improved in these 3-pyridinols by virtue of their increased ionization potential (IP) compared to that of phenols.⁹



We have prepared a series of *C*(7)-mono- and dialkyl tetrahydro-1,8-naphthyridinols structurally similar to α -TOH and its truncated *C*(2) side-chain analogue, 2,2,5,7,8-pentamethyl-6-chromanol (PMC). The phytol-derived side chain of α -TOH and its substitution pattern play an important role in the (re)-absorption and delivery of α -TOH to lipoproteins,^{10,11} and it seems reasonable to assume that *C*(7) substitution will provide a suitable platform for physiologically relevant analogues of this core structure for studies *in vivo*.

Substitution at *C*(7) may also affect pyridinoxyl radical stability and hence the antioxidant activity.^{6,12} The electron lone pair of the para N(8) atom should be oriented perpendicular to the aromatic ring plane for maximum orbital overlap. The rate constants for inhibition by **5** and **6** demonstrate this stereoelectronic effect.¹² Although the greater electron-donating effect of N compared to O suggests a better k_{inh} for **6** than for **5**, the actual k_{inh} for **6** ($2.0 \times 10^6 \text{ M}^{-1} \text{ s}^{-1}$) is smaller than that of **5** ($2.7 \times 10^6 \text{ M}^{-1} \text{ s}^{-1}$) because of steric interactions between the *N*-ethyl group and the *C*(8)-methyl. Substitution at *C*(7) of the naphthyridinols may well affect the orientation of the N(8) lone pair.



We report herein the synthesis of naphthyridinols with various alkyl side chains, including a *C*(7)-dialkyl naphthyridinol with the α -TOH side chain, which we will refer to as N-TOH. We also report a study of the stereoelectronic effect of substitution on the naphthyridinol core structure by measurement of inhibition rate constants. In addition, we moved toward *in vivo* studies of this interesting class of compounds by testing the efficacy of N-TOH as an inhibitor of low-density lipoprotein (LDL) oxidation,^{13–16} studying the lateral diffusion of this compound in a model membrane system (1-palmitoyl-2-oleoyl-*sn*-glycero-3-phosphocholine liposomes) and determining its

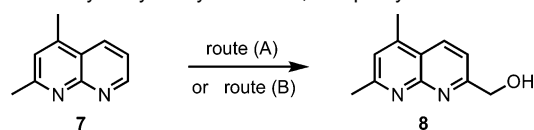
- (9) Pratt, D. A.; DiLabio, G. A.; Brigati, G.; Pedulli, G. F.; Valgimigli, L. *J. Am. Chem. Soc.* **2001**, *123*, 4625–4626.
(10) Traber, M. G.; Ramakrishnan, R.; Kayden, H. J. *Proc. Natl. Acad. Sci. U.S.A.* **1994**, *91*, 10005–10008.
(11) Traber, M. G. *Free Radical Biol. Med.* **1994**, *16*, 229–239.
(12) Burton, G. W.; Doba, T.; Gabe, E. J.; Hughes, L.; Lee, F. L.; Prasad, L.; Ingold, K. U. *J. Am. Chem. Soc.* **1985**, *107*, 7053–7065.

ability to bind to the human tocopherol transfer protein (hTTP).^{11,17} In each of these studies, N-TOH shows performance that is comparable to or improved over that of the natural compound, α -TOH.

Results and Discussion

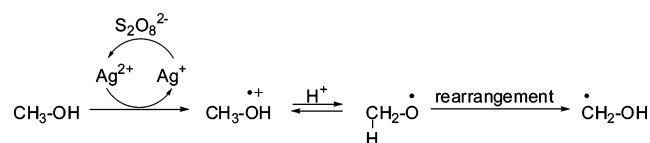
Synthesis of *C*(7)-Alkylated Naphthyridinols. We reported previously that naphthyridinol antioxidants can be synthesized from 1,8-naphthyridine **7**. A quaternary carbon center was constructed at *C*(7) by alkyllithium addition to 1,8-naphthyridine **8**, which was synthesized by the five-step reaction sequence as shown in Scheme 1 (route A).¹⁸ The hydroxymethyl functionality is key, since once it is protected as the *t*-butyldimethylsilyl (TBS) ether as in **9**, it serves to direct the alkyllithium addition into the right ring through five-membered cyclic chelation in nonpolar solvents.¹⁸

Scheme 1. Hydroxymethylation of 1,8-Naphthyridine **7**^a



^a Route A:¹⁸ (i) CH₂=CHMgBr, (ii) MnO₂, (iii) OsO₄, (iv) NaO₄, (v) NaBH₄, overall 60%. Route B: AgNO₃, (NH₄)₂S₂O₈, H₂SO₄, MeOH, reflux, 1.5 h, 88%.

An improved synthesis of **8** from **7** can be achieved by a modification of a literature protocol.¹⁹ It was reported that a hydroxymethyl radical ($\cdot\text{CH}_2\text{OH}$) can be added to heteroaromatics such as quinolines by a procedure involving refluxing ethylene glycol in the presence of silver nitrate (AgNO₃), ammonium persulfate ((NH₄)₂S₂O₈), and trifluoroacetic acid (TFA). We found that this procedure, where ethylene glycol is the source of hydroxymethyl radical, afforded virtually no reaction for **7**. In fact, **7** requires milder conditions where MeOH is the hydroxymethyl radical source. Refluxing **7** in MeOH with silver nitrate, ammonium persulfate and sulfuric acid afforded **8** in high yield (88%; Scheme 1, route B). No significant amount of aldehyde, dearomatized, or *N*-oxidation products were observed under these conditions. The addition of TFA (Table 1, entry 3) or water (entry 2) to the reaction mixture resulted in either lower yield or more degradation. An excess of (NH₄)₂S₂O₈ (entry 4) was also detrimental to the reaction, leading to a lower yield. The mechanism of hydroxymethyl radical formation is shown below.

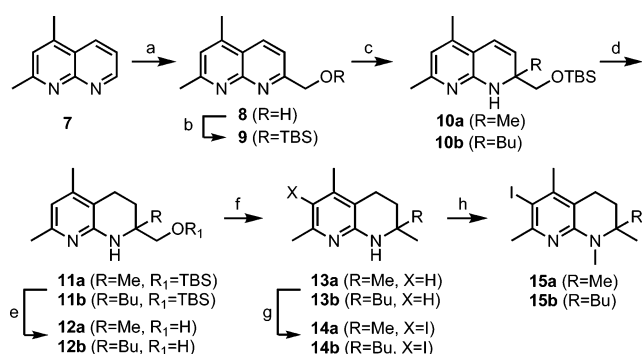


- (13) Kim, H. Y.; Pratt, D. A.; Seal, J. R.; Wijtman, M.; Porter, N. A. *J. Med. Chem.* **2005**, *48*, 6787–6789.
(14) Bowry, V. W.; Ingold, K. U.; Stocker, R. *Biochem. J.* **1992**, *288*, 341–344.
(15) Bowry, V. W.; Ingold, K. U. *Acc. Chem. Res.* **1999**, *32*, 27–34.
(16) Gotoh, N.; Noguchi, N.; Tsuchiya, J.; Morita, K.; Sakai, H.; Shimasaki, H.; Niki, E. *Free Radical Res.* **1996**, *24*, 123–134.
(17) Kaempf-Rotzoll, D. E.; Traber, M. G.; Arai, H. *Curr. Opin. Lipids* **2003**, *14*, 249–254.
(18) Nam, T. G.; Wijtman, M.; Pratt, D. A.; Porter, N. A. *Synthesis* **2005**, 1397–1404.
(19) Minisci, F.; Porta, O.; Recupero, F.; Punta, C.; Gambarotti, C.; Pruna, B.; Pierini, M.; Fontana, F. *Synlett* **2004**, 874–876.

Table 1. AgNO₃-Catalyzed Hydroxymethylation^a of 1,8-Naphthyridine **7**

entry	solvent	acid (equiv)	(NH ₄) ₂ S ₂ O ₈	yield (%) ^b
1	(CH ₂ OH) ₂ /H ₂ O (1/1)	TFA	4.0	no rxn
2	MeOH/H ₂ O (5/1)	H ₂ SO ₄ (1.0)	4.0	46
3	MeOH	TFA (2.0)	4.0	72
4	MeOH	H ₂ SO ₄ (1.2)	6.0	63
5	MeOH	H ₂ SO ₄ (0.7)	2.8	88

^a Reaction was refluxed for 1.5 h in all cases. Prolonged reaction time did not increase the yield. ^b Measured by ¹H NMR of crude reaction mixture, except for entry 5 (isolated yield).

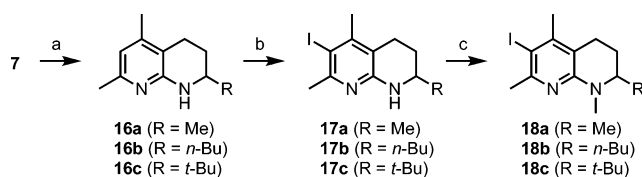
Scheme 2^a

^a Reagents and conditions: (a) AgNO₃, (NH₄)₂S₂O₈, H₂SO₄, MeOH, reflux, 1.5 h, 88%; (b) TBSCl, DMAP, Et₃N, CH₂Cl₂, room temperature, overnight, 93%; (c) R-Li (R = Me, *n*-Bu), LiBr, Et₂O/hexanes (1/2), 0 °C, 1 h, 75% (**10a**), 71% (**10b**); (d) Pd/C, H₂, MeOH, room temperature, overnight, 88% (**11a,b**); (e) TBAF, THF, room temperature, 1 h, 96% (**12a,b**); (f) (i) PPh₃, I₂, imidazole, CH₂Cl₂, room temperature, 1.5 h, (ii) Zn dust, AcOH, 70 °C, 1 h, 78% (**13a**), 75% (**13b**); (g) NIS, TFA, CH₃CN, room temperature, 3.5 h, 92% (**14a**), 93% (**14b**); (h) HCHO(aq), NaCNBH₃, AcOH, MeOH, room temperature, 3.5 h, 94% (**15a**), 92% (**15b**).

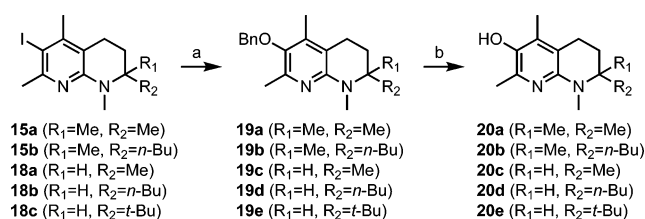
Silver(I) ion is oxidized by persulfate to silver(II), which then oxidizes methanol to its radical cation. The weak C–H bond prompts a rearrangement to form a carbon-centered radical. Since the ring nitrogens of **7** are protonated under strongly acidic conditions, a hydroxymethyl radical can be added to C(7). Regioselectivity for radical addition to C(7) over C(2) of **7** has precedent in other radical addition reactions, which are known to be subject to steric effects.

The synthesis of C(7)-dialkyl-substituted naphthyridinols is summarized in Scheme 2. Alkylolithiums (*n*-BuLi and MeLi) were regioselectively added to **9**. The desired regioisomers were obtained in 71–75% isolated yields. The dihydronaphthyridines **10** were subsequently hydrogenated to afford tetrahydronaphthyridines **11**, from which the TBS group was removed with tetrabutylammonium fluoride (TBAF) to give **12** in 96% yield. The alcohol function of **12** was reductively cleaved to afford **13** in 75–78% yield via the corresponding iodide intermediate. Iodination of the pyridine ring of **13** was carried out with *N*-iodosuccinimide (NIS) in the presence of a catalytic amount of TFA²⁰ to afford **14** in 92–93% yield. Iodination using either I₂ or NIS alone gave lower yields (40–60%). *N*-Methyl **15** was, then, obtained by reductive alkylation in 92–93% yield.

C(7)-Monoalkyl compounds were also synthesized from 1,8-naphthyridine **7**. Alkylolithiums (MeLi, *n*-BuLi, and *t*-BuLi) were added to the unsubstituted C(7)-position of **7**. After regioselective alkylolithium addition, reduction of the remaining double

Scheme 3^a

^a Reagents and conditions: (a) (i) R-Li (R = Me, *n*-Bu, *t*-Bu), LiBr, Et₂O, 0 °C, 1 h; (ii) Pd/C, H₂, MeOH, room temperature, overnight, 63–68%; (b) NIS, TFA, CH₃CN, room temperature, 4–5 h, 92–95%; (c) HCHO(aq), NaCNBH₃, AcOH, MeOH, room temperature, 4–6 h, 88–91%.

Scheme 4^a

^a Reagents and conditions: (a) (i) CuI, Cs₂CO₃, BnOH, 90 °C, 2 days, 72–81%; (b) Pd/C, H₂, MeOH, room temperature, 3.5 h, 92–97%.

bond in the dihydronaphthyridines was carried out immediately to give **16**, because the dihydronaphthyridine intermediates are labile toward rearomatization when C(7) is not fully substituted. The same conditions as described in Scheme 2 were applied thereafter to afford the C(7)-monoalkyl iodo compounds **18** (Scheme 3).

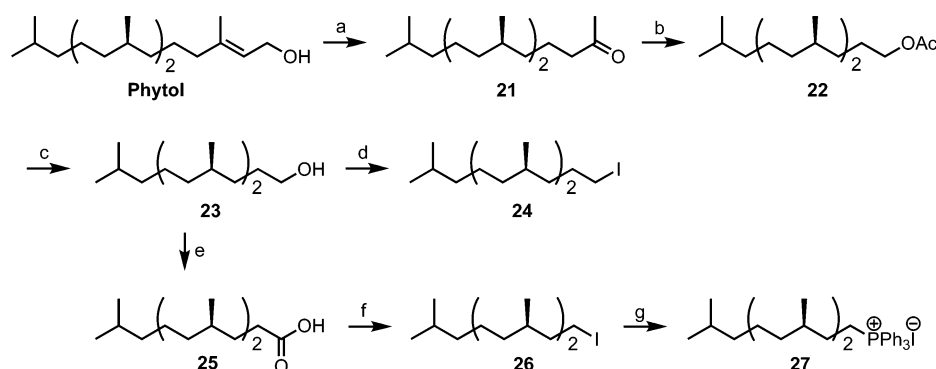
Several approaches were explored to convert iodides **15** and **18** to the corresponding naphthyridinols, and in our hands benzyloxylation of the aryl iodide under CuI-mediated benzyloxylation conditions,^{21,22} followed by hydrogenolysis was the preferred method. Benzyloxylation of the corresponding bromo precursors or the N(8)H free amino precursors gave low yields. Addition of a catalytic amount of 1,10-phenanthroline²² did not give a significant improvement in yield. After benzyloxylation, the benzyl groups of compounds **19a–e** were then removed by catalytic hydrogenolysis to give the final naphthyridinols **20a–e** (Scheme 4). This benzyloxylation–hydrogenolysis reaction sequence is especially advantageous in that (i) the hydrogenolysis conditions keep naphthyridinol antioxidants, which decompose over a period of days when exposed to the air, from degradation during and after the deprotection reaction; (ii) chromatographic purification, which is unavoidable in our previous 2-nitro-*m*-xylene oxygenation method^{7,8,18} and a possible source of air oxidation, is not necessary once the catalyst is removed by filtration; and (iii) the yield of the hydroxylation is significantly higher than that from 2-nitro-*m*-xylene (<30%). This protocol is not only highly efficient but is also simple and safe for air-sensitive antioxidants such as **20a–e** (Scheme 4).

Synthesis of N-TOH. Distribution of α -TOH to tissues by the tocopherol transfer protein (TTP)¹⁷ and other tocopherol binding proteins (TBP) relies on recognition of ring methyl groups, configuration at the ring stereogenic center, and the C₁₆ side chain.^{23–25} It has been suggested that this recognition plays an important role in the (re)absorption and delivery of α -TOH

(20) Castanet, A. S.; Colobert, F.; Broutin, P. E. *Tetrahedron Lett.* **2002**, *43*, 5047–5048.

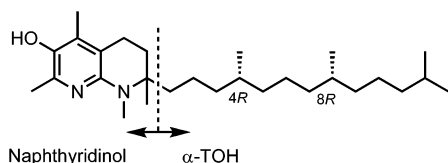
(21) Job, G. E.; Buchwald, L. *Org. Lett.* **2002**, *4*, 3703–3706.

(22) Wolter, M.; Nordmann, G.; Job, G. E.; Buchwald, S. L. *Org. Lett.* **2002**, *4*, 973–976.

Scheme 5^a

^a Reagents and conditions: (a) KMnO_4 , acetone, room temperature, 3 h, 72%; (b) TFAA, $\text{Na}_2\text{CO}_3 \cdot 1.5\text{H}_2\text{O}$, CH_2Cl_2 , room temperature, overnight; (c) LiOH , $\text{THF}/\text{MeOH}/\text{H}_2\text{O}$, room temperature, 2 h, 92% for two steps; (d) PPh_3 , imidazole, I_2 , 0°C , 40 min, 90%; (e) $\text{RuCl}_3 \cdot x\text{H}_2\text{O}$, NaIO_4 , $\text{CCl}_4/\text{CH}_3\text{CN}/\text{H}_2\text{O}$, room temperature, 5 h, 87%; (f) $\text{PhI}(\text{OAc})_2$, I_2 , $h\nu$, CCl_4 , 65°C , 4 h, 86%; (g) PPh_3 , toluene, 110°C , 5 h, quantitative.

to tissues and its incorporation into LDL particles,^{10,25,44} while antioxidant activity against the oxidation of isolated LDL was inversely proportional to the length of the side chain of the α -TOH analogue.^{15,16} Therefore, we set out to hybridize the naphthyridinol antioxidant core with α -TOH's C_{16} -isoprenoid side chain to prepare more physiologically relevant analogues.²⁵

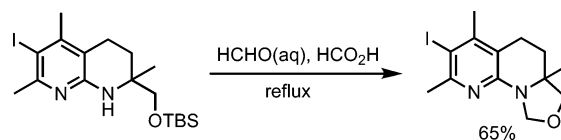


Attachment of the C_{16} chain can be achieved either by C_{16} -Li addition, as shown in Scheme 2 for BuLi or MeLi , or by Wittig olefination with a C_{15} ylide (Scheme 5). The configuration of the stereogenic centers in the C_{16} chain can be obtained from the chiral pool in the form of the C_{20} natural product

phytol, which has the same configuration as does the α -TOH side chain. In the R-Li addition approach, C_{16} -Li was prepared *in situ* from **24** and $t\text{-BuLi}$ ²⁶ and added to the naphthyridine **9**. Unlike MeLi and $n\text{-BuLi}$, C_{16} -Li afforded the addition product in low yield, 21%. Alternatively, the side chain could be attached to the naphthyridinol core by a Wittig coupling, which required the C_{15} ylide **27** and the naphthyridine aldehyde **31**.

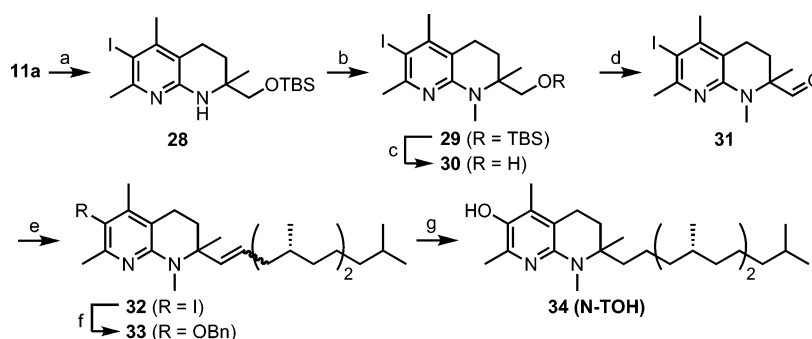
For the synthesis of **27**, phytol was oxidatively cleaved to the methyl ketone **21** with KMnO_4 ²⁷ in 72% yield. As expected from the extremely low migratory ability of a primary alkyl group under Baeyer–Villiger conditions, reactions of **21** with conventional oxidants such as $m\text{-CPBA}$ gave no Baeyer–Villiger product. The best-known conditions for primary alkyl group migration, including 50% H_2SO_4 with $\text{K}_2\text{S}_2\text{O}_8$,²⁸ were not successful, presumably due to the poor solubility of such a lipophilic compound in aqueous medium. Addition of a detergent such as Triton X-305 improved the conversion but made the isolation of the product difficult. A Baeyer–Villiger reaction on **21** was, however, achieved in very high yield with trifluoroacetic acid generated *in situ* from trifluoroacetic acid anhydride and sodium percarbonate.²⁹ Subsequent hydrolysis of the acetyl group with LiOH gave the C_{16} alcohol **23** in 92% for two steps. The carboxylic acid **25** was obtained from **23** by reaction with ruthenium(III) chloride in 87% yield. A radical-mediated tandem decarboxylation–iodination reaction with iodosobenzene diacetate³⁰ and I_2 converted the acid **25** to C_{15} -iodide **26** in 86% yield. The phosphonium salt **27** was prepared from reaction with PPh_3 in toluene as a yellow solid.

For the synthesis of naphthyridine aldehyde **31** (Scheme 6), **11a** underwent iodination and reductive N -methylation to give **29** according to the conditions described in Scheme 2. Interestingly, N -methylation of **28** under Escheweiler–Clark conditions resulted in tricyclic compounds.



Removal of the TBS group in **29** with TBAF gave the alcohol **30**, which was then oxidized to the aldehyde **31** in 78% yield with Dess–Martin periodinane. Wittig coupling with phosphonium salt **27** was surprisingly smooth, despite that aldehyde **31** may suffer from neopentyl-type steric hindrance. Subsequently,

- (23) Stocker, A.; Zimmer, S.; Spycher, S. E.; Azzi, A. *IUBMB Life* **1999**, *48*, 49–55.
 (24) Munteanu, A.; Zingg, J. M.; Azzi, A. J. *Cell Mol. Med.* **2004**, *8*, 59–76.
 (25) Traber, M. G.; Kayden, H. J. *Am. J. Clin. Nutr.* **1989**, *49*, 517–526.
 (26) Bailey, W. F.; Punzalan, E. R. *J. Org. Chem.* **1990**, *55*, 5404–5406.
 (27) Mizuguchi, E.; Takemoto, M.; Achiwa, K. *Tetrahedron: Asymmetry* **1993**, *4*, 1961–1964.
 (28) Deno, N. C.; Billups, W. E.; Kramer, K. E.; Lastomirsky, R. R. *J. Org. Chem.* **1970**, *35*, 3080.
 (29) Kang, H. J.; Jeong, H. S. *Bull. Kor. Chem. Soc.* **1996**, *17*, 5–6.
 (30) Concepcion, J. I.; Francisco, C. G.; Freire, R.; Hernandez, R.; Salazar, J. A.; Suarez, E. *J. Org. Chem.* **1986**, *51*, 402–404.
 (31) Peroxidation of γ -linolenate and arachidonate esters: Rector, C. L.; Stec, D. F.; Brash, A. R.; Porter, N. A. *Chem. Res. Toxicol.*, in press.
 (32) Roschek, B.; Tallman, K. A.; Rector, C. L.; Gillmore, J. G.; Pratt, D. A.; Punta, C.; Porter, N. A. *J. Org. Chem.* **2006**, *71*, 3527–3532.
 (33) A double-reciprocal plot can also be used to analyze the data, as reported in ref 31.
 (34) Sonnen, A. F. P.; Bakirci, H.; Netscher, T.; Nau, W. M. *J. Am. Chem. Soc.* **2005**, *127*, 15575–15584.
 (35) Gramlich, G.; Zhang, J.; Nau, W. M. *J. Am. Chem. Soc.* **2004**, *126*, 5482–5492.
 (36) Nau, W. M. *J. Am. Chem. Soc.* **1998**, *120*, 12614–12618.
 (37) Pischel, U.; Patra, D.; Koner, A. L.; Nau, W. M. *Photochem. Photobiol.* **2006**, *82*, 310–317.
 (38) Niki, E.; Noguchi, N. *Acc. Chem. Res.* **2004**, *37*, 45–51.
 (39) Niki, E.; Kawakami, A.; Saito, M.; Yamamoto, Y.; Tsuchiya, J.; Kamiya, Y. *J. Biol. Chem.* **1985**, *260*, 2191–2196.
 (40) Shi, H.; Noguchi, N.; Niki, E. *Free Radical Biol. Med.* **1999**, *27*, 334–346.
 (41) Barclay, L. R. C.; Ingold, K. U. *J. Am. Chem. Soc.* **1981**, *103*, 6478–6485.
 (42) Nava, P.; Cecchini, M.; Chirico, S.; Gordon, H.; Morley, S.; Manor, D.; Atkinson, J. *Bioorg. Med. Chem.* **2006**, *14*, 3721–3736.
 (43) We know that aqueous solutions of α -TOH are likely not true solutions, and we have always observed poor competition (or other behaviours) at high concentrations of α -TOH.
 (44) Panagabko, C.; Morley, S.; Hernandez, M.; Cassolato, P.; Gordon, H.; Parsons, R.; Manor, D.; Atkinson, J. *Biochemistry* **2003**, *42*, 6467–6474.

Scheme 6^a

^a Reagents and conditions: (a) NIS, TFA, CH₃CN, room temperature, 3 h, 87%; (b) HCHO(aq), NaCNBH₃, AcOH, MeOH/THF, room temperature, overnight, 85%; (c) TBAF, THF, room temperature, 12 h, 92%; (d) Dess–Martin Periodinane, CH₂Cl₂, room temperature, 1 h, 78%; (e) **27**, *n*-BuLi, THF, 0 °C, 1 h, then **31**, room temperature, 2 h, 85%; (f) CuI, Cs₂CO₃, BnOH, 90 °C, 2 days, 78%; (g) Pd/C, H₂, EtOH, room temperature, 2 days, 94%.

CuI-mediated benzyloxylation was carried out on the Wittig product **32** to give benzyl-protected hydroxy product **33**. It is noteworthy that scrambling the reaction sequence from **29** to **33** dramatically reduces the overall yield. Oxidation of alcohol **30** to the aldehyde **31** and Wittig coupling should be carried out prior to the benzyloxylation. Otherwise, oxidation of the benzyloxy-containing alcohol compound to the corresponding aldehyde results in significant degradation along with low yield (32%). In order to afford naphthyridinol-based tocopherol (N-TOH) **34**, both the benzyl group and the double bond of **33** were removed at the same time under catalytic hydrogenation conditions.

Antioxidant Activity in Benzene: Determination of k_{inh} .

The inhibition rate constant (k_{inh}) of the representative naphthyridinols, which corresponds to the rate constant for H-atom transfer to the chain-carrying peroxy radicals in lipid peroxidation, was measured by a peroxy radical clock system based on the autoxidation of pentafluorobenzyl 13(*S*)-hydroxyoctadeca-6*Z*,9*Z*,11*E*-trienoate (13-HOTrE).³¹ This radical clock is similar to the linoleate peroxy radical clocks previously described, but relies on the assistance of mass spectrometry for product analysis.³² This clock is based on the competition between trapping the kinetically favored 8-hydroperoxy, 13-(*S*)-6*Z*,9*Z*,11*E*-trienoate (8,13-*c,c,t*) versus peroxy radical β -fragmentation that leads to other, thermodynamically more stable products. This system gives good values of k_{inh} , as has been established with antioxidants having known k_{inh} values.³¹

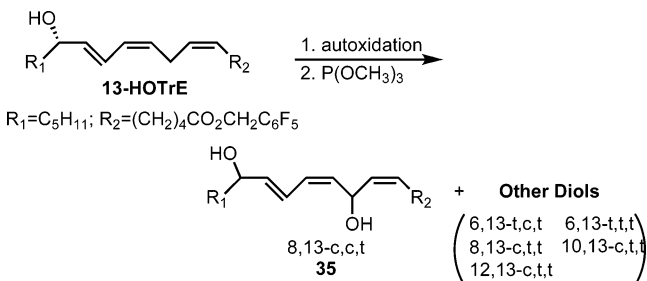


Figure 1 shows data obtained from the oxidation of 13-HOTrE in the presence of varying amounts of α -tocopherol. The value of $\text{KP} = k_{\text{inh}}(\alpha\text{-TOH})[\alpha\text{-TOH}]$ is plotted vs the ratio of the 8,13-dihydroxy-6*Z*,9*Z*,11*E*-octadecatrienoate **35** to the other dihydroxy products formed from oxidation of 13-HOTrE. The product **35** is not observed for oxidations of 13-HOTrE carried out in the absence of tocopherol, but it is formed in an increasing

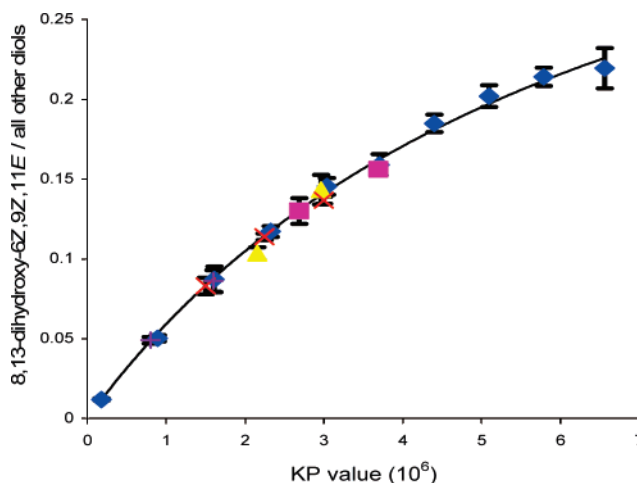
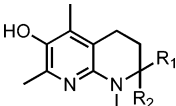
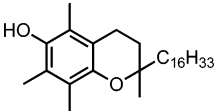


Figure 1. Plot of diol product ratio from oxidation of 13-HOTrE in the presence of α -tocopherol and naphthyridinols **1** and **20a,c,e**. KP values were derived from the measurements of k_{inh} of the bicyclic antioxidants using the triene clock: $\text{KP} = [\text{H-donor}]k_{\text{inh}}^{\text{donor}}$. Blue \blacklozenge , α -TOH; red \times , **1**; yellow \blacktriangle , **20a**; pink \blacksquare , **20c**; violet $+$, **20e**. Typical reaction mixture contains 100 mM starting material (13-HOTrE), 2.5 mM 2,2'-azobis(4-methoxy-2,4-dimethylvaleronitrile) (MeOAMVN), and 40–80 mM antioxidant in benzene. The reaction mixture was incubated at 37 °C for 1 h. After the incubation, hydroperoxides were reduced by $\text{P}(\text{OCH}_3)_3$. Rate constants were determined as the ratio between the kinetic product (8,13-*c,c,t*) and the remaining products (the other diols).

amount as the concentration of antioxidant is increased. The curve in Figure 1, obtained for α -TOH, establishes the product response to different concentrations of an antioxidant having a known inhibition rate constant, $k_{\text{inh}}(\alpha\text{-TOH})$. To determine the k_{inh} of other antioxidants, oxidation of 13-HOTrE is carried out in the presence of several known concentrations of those antioxidants, and the product ratio of **35** to all other diols is determined by HPLC/MS/MS. Fitting the product ratio observed for an antioxidant having an unknown k_{inh} on the product–KP plot shown in Figure 1 permits determination of KP for the antioxidant under given conditions. $\text{KP} = k_{\text{inh}}[\text{Inh}]$ for any inhibitor and $[\text{Inh}]$ is known for any given experiment, making determination of k_{inh} possible. Product ratios from oxidation of 13-HOTrE in the presence of the naphthyridinols **1** and **20a,c,e** were used to determine k_{inh} for those antioxidants, and the results of those studies are presented in Table 2.³³

As shown in Table 2, all of the naphthyridinol antioxidants are better hydrogen atom donors than α -TOH, with k_{inh} values at least 15-fold higher than that of α -TOH. *C*(7)-Alkyl substitution does not generate significant differences in their antioxidant

Table 2. Inhibition Rate Constants (k_{inh}) Measured in Benzene at 37 °C by the 13-HOTrE Radical Clock^a

compound	k_{inh} ($\times 10^7 \text{ M}^{-1} \text{ s}^{-1}$)	$k_{\text{inh}}/$ $k_{\text{inh}}(\alpha\text{-TOH})$
 20c ($R_1 = \text{H}, R_2 = \text{Me}$)	6.1 ± 0.7	17
20e ($R_1 = \text{H}, R_2 = t\text{-Bu}$)	5.7 ± 0.7	16
20a ($R_1 = \text{Me}, R_2 = \text{Me}$)	5.2 ± 0.8	15
1b ($R_1 = \text{H}, R_2 = \text{H}$)	5.3 ± 0.6	15
 $\alpha\text{-TOH}$	0.35	1.0

^a See caption for Figure 1. Errors are ± 1 SD. ^b k_{inh} of **1** was reported⁷ to be $(8.8 \pm 3.2) \times 10^7 \text{ M}^{-1} \text{ s}^{-1}$.

activities within the error range of about 10%. Steric interactions between the *N*(8)-methyl and *C*(7)-alkyl group are apparently tolerable and do not create significant stereoelectronic effects. In line with these results, differences in the dihedral angles of these compounds, calculated by MM2 molecular dynamics, are also subtle (data not shown). It is notable that the k_{inh} value of unsubstituted **1** was slightly lower than those of substituted naphthyridinols **20**. This same trend was found in chromanol analogues:¹² dimethyl-substituted PMC ($k_{\text{inh}} = 3.8 \times 10^6 \text{ M}^{-1} \text{ s}^{-1}$) versus unsubstituted analogue **5** ($k_{\text{inh}} = 2.7 \times 10^6 \text{ M}^{-1} \text{ s}^{-1}$).

Lateral Diffusion in Model Membranes. The propensity of an antioxidant to donate hydrogen atoms to reactive species provides an important measure of its reactivity. Relative hydrogen donor propensities can be directly assessed by a time-resolved spectroscopic technique that involves the fluorescence quenching of 2,3-diazabicyclo[2.2.2]oct-2-ene in benzene.^{34–37} The fluorescence quenching rate constant (k_{q}) of N-TOH in benzene ($k_{\text{q}} = (5.4 \pm 0.5) \times 10^9 \text{ M}^{-1} \text{ s}^{-1}$; this work) was found to be very similar to the value determined for $\alpha\text{-TOH}$ ($k_{\text{q}} = (5.3 \pm 0.3) \times 10^9 \text{ M}^{-1} \text{ s}^{-1}$; ref 34), and both values lie close to the diffusion-controlled limit. This demonstrates that N-TOH is an exceptionally reactive hydrogen atom donor, as good as or better than $\alpha\text{-TOH}$, which itself is the best hydrogen donor among the vitamin E constituents.³⁴

The activity of antioxidants in membrane environments is affected to a large degree by the mobility and accessibility of the antioxidant.^{38–41} We have assessed the mobility of N-TOH in membrane models with a recently established fluorescence quenching method, which employs the azoalkane Fluorazophore-L, a palmitoyl derivative of 2,3-diazabicyclo[2.2.2]oct-2-ene, as a fluorescent probe for antioxidants. This method, which has been established for vitamin E constituents,^{34,35} affords effective lateral diffusion coefficients. Fluorescence decay traces of Fluorazophore-L in 1-palmitoyl-2-oleoyl-*sn*-glycero-3-phosphocholine liposomes at varying N-TOH concentrations (see Supporting Information) were recorded at different temperatures, and the effective mutual lateral diffusion coefficients (D_{L}) were recovered by global fitting (Table 3). Comparison with the values previously obtained for $\alpha\text{-TOH}$ ^{34,35} showed slightly larger D_{L} values for N-TOH, but the error was larger due to interference from fluorescence of N-TOH. The activation energy for fluorescence quenching of Fluorazophore-L by N-TOH ($43 \pm 6 \text{ kcal/mol}$) was found to be the same, within error, as that observed for $\alpha\text{-TOH}$ ($47 \pm 5 \text{ kcal/mol}$). Such activation energies

Table 3. Mutual Lateral Diffusional Coefficient of N-TOH in 1-Palmitoyl-2-oleoyl-*sn*-glycero-3-phosphocholine Liposomes

temp (°C)	D_{L} ($10^{-7} \text{ cm}^2 \text{ s}^{-1}$)	
	N-TOH ^a	$\alpha\text{-TOH}^b$
20	1.8	1.1 ^c
25	2.3	1.54
30	3.1	2.10
40	5.4	3.73
50	9.0	6.42

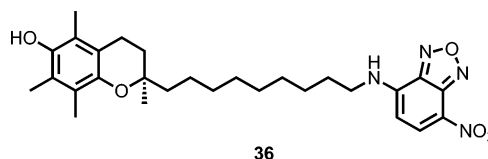
^a 20% error. ^b 10% error, from ref 34. ^c Interpolated value.

are characteristic for laterally diffusion-controlled reactions in 1-palmitoyl-2-oleoyl-*sn*-glycero-3-phosphocholine liposomes.³⁴

The absolute D_{L} values determined by the fluorescence quenching method are modulated by an efficiency factor, which reflects the accessibility of the excited fluorophore by the reactive site of the antioxidant, i.e., the transversal positioning within the lipid leaflet. Variations of this efficiency factor need to be considered when (i) the hydrogen donor propensities of two antioxidants are comparable and (ii) the activation energies are both comparable to that of the solvent viscous flow of the lipid but (iii) significant variations in the absolute D_{L} values are observed. The smaller D_{L} values previously obtained for ascorbyl palmitate relative to those for tocopherols, for example, have been attributed to a *less favorable* positioning within the lipid, namely a displacement toward the aqueous phase due to the anionic ascorbyl head group.³⁴ Conversely, the slightly larger effective D_{L} values for N-TOH than for $\alpha\text{-TOH}$ (Table 3) are tentatively attributed to *more favorable* transversal positioning in the membrane, possibly a deeper penetration due to a lower polarity or weaker hydrogen-bonding propensity of N-TOH.

Binding to Human Tocopherol Transfer Protein (TTP).

Tocopherol transfer protein (TTP) plays an important role in the transport of $\alpha\text{-tocopherol}$ in tissues and fluids in the body. To examine whether N-TOH is a substrate for TTP, we used it to displace a fluorescent $\alpha\text{-tocopherol}$ analogue (NBD-Toc, **36**)⁴² from the recombinant human protein and compared the result to the ability of $\alpha\text{-TOH}$ to do the same.



As shown in Figure 2, N-TOH is actually a better competitor for the bound fluorophore (NBD-Toc) than is $\alpha\text{-TOH}$. In fact,

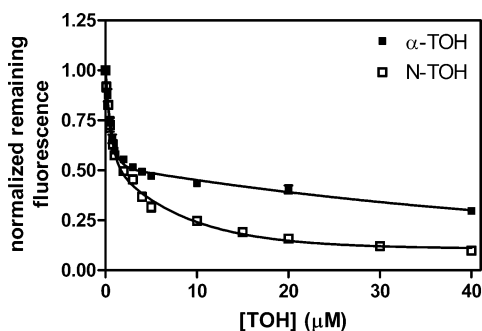


Figure 2. Competition of TTP-bound NBD-Toc with α -TOH (■) and N-TOH (□). The assay was done as follows: recombinant human TTP (0.2 μM) was incubated with 1.0 μM NBD-Toc in SET buffer (250 mM sucrose, 1 mM EDTA, 50 mM Tris, pH 7.4) containing 20 μM Triton X-100 at ~ 20 °C. The fluorescence of NBD-Toc is greatly enhanced on binding to the protein. After the signal reached equilibrium, small aliquots of competitor dissolved in EtOH were added, and the signal was observed until any observed fluorescence decrease came to a steady value. Graphs were made in the Prism software package and are best fit to a two-phase exponential decay, although the reasons for that are not obvious.

after addition of N-TOH to the protein–fluorophore mixture, the fluorescence eventually drops to the background value for NBD-Toc in aqueous solution at this concentration. N-TOH decreased the fluorescence of TTP/NBD-Toc to 50% of the original intensity at about 2 μM . Under the conditions of the assay, α -TOH required about 3.2 μM to reach the same point.⁴³ From the fluorescent titration of TTP with NBD-Toc, we calculate a dissociation constant (K_d) of about 30–60 nM. By way of comparison, a radioligand binding assay with ^3H - α -TOH gives a K_d of 25 nM for α -TOH binding to TTP,⁴⁴ which demonstrates the validity of this fluorescence assay.

An examination of the X-ray crystallographic structure of α -TOH bound to recombinant hTTP (PDB code 1OIP)⁴⁵ allows us to rationalize this observation (Figure 3). Recall the two structural differences between α -TOH and N-TOH are (1) the C(8)-methyl group of α -TOH is replaced by a nitrogen lone pair in N-TOH and (2) the chroman ring oxygen atom of α -TOH is replaced by a N–CH₃ moiety in N-TOH. The first substitution results in the loss of the van der Waals contacts between the C(8)-methyl group of α -TOH and the nearest carbon atoms on the side chains of Ile-137, Val-182, and Phe-133 of the TTP active site (positioned 3.9, 3.7, and 3.9 Å, respectively, from the carbon atom of the C(8)-methyl carbon atom, Figure 3a). However, this loss is likely made up for and more by an H-bond between the nitrogen lone pair of the N–CH₃ moiety and the hydroxyl of Ser-136 (Figure 3b). The CH₂ group of Ser-136 makes a close contact of 3.2 Å with the chroman ring O atom in the α -TOH/hTTP X-ray crystal structure,⁴⁵ in which it is H-bonded to a water molecule, and simply flipping the Ser-136 side chain to its other rotamer brings the Ser oxygen to within 2.7 Å of the chroman O. Given that the amine nitrogen is a far better H-bond acceptor than either water or the chroman ring oxygen, it is highly likely that this would be the preferred conformation of Ser-136 for binding N-TOH and may account for the preferential binding of N-TOH to the TTP compared to α -TOH. It should be noted that N-TOH was assayed as a racemic mixture of the (*SRR*) and (*RRR*) stereoisomers. If (*SRR*)-N-TOH is as relatively poor a ligand as (*SRR*)- α -TOH (545 nM versus 25 nM for (*RRR*)- α -TOH), then the (*RRR*)-N-TOH

binds even better than it would appear in Figure 2, since only half the sample is effectively competing with NBD-Toc for the active site. There would appear to be ample space for the methyl group of the N–CH₃ moiety in the hydrophobic pocket formed by Phe-133, Ile-137, and Val-182, since the C–C distances are all >3 Å without changing rotamer conformations or energy-minimizing the model.

Inhibition of Lipid Peroxidation in LDL Particles. LDL oxidation has been proposed to play a central role in the early development of atherosclerosis.^{3,4} It has been known for some time that α -TOH is not a particularly good antioxidant in LDL.¹⁴ In the absence of co-antioxidants such as ascorbate (vitamin C) and reduced coenzyme Q₁₀, supplementation of LDL with α -TOH increases the oxidation of cholesteryl linoleate and phospholipids. It was speculated that α -TOH mediates lipid peroxidation through antioxidant (tocopherol)-mediated peroxidation (AMP (TMP)),¹⁴ where a tocopheroxyl radical abstracts a hydrogen atom from a lipid molecule (LH) to generate L•, a chain-carrying radical. However, this process is quite slow ($k_{\text{TMP}} = 0.1 \text{ M}^{-1} \text{ s}^{-1}$).

In contrast, lipophilic naphthyridinol **2** inhibits the oxidation of cholesteryl linoleate (Chol-Lin) in human LDL, spares endogenous α -TOH, and does not promote AMP of lipid.¹³ This prompted us to examine whether **34**, which is structurally more closely related to α -TOH than is **2**, shows good antioxidant behavior in LDL oxidation.

Freshly obtained plasma was incubated for 1.5 h at 37 °C, with or without N-TOH. Oxidation of the LDL isolated using sequential centrifugations was initiated by 2,2-azobis[2-(2-imidazolin-2-yl)propane-2-yl]dihydrochloride (AIPH) according to literature procedure.¹³ Figure 4 plots the formation of oxidation products from cholesteryl linoleate and the remaining antioxidant (AOX): N-TOH and α -TOH. Without supplementation of N-TOH, the endogenous α -TOH level decreases instantly as the oxidation proceeds, providing no protection against the oxidation of Chol-Lin (Figure 4A). On the other hand, supplementation of N-TOH (75 μM final concentration) resulted in a dramatic change in the oxidation profile (Figure 4B).¹³ N-TOH efficiently protects Chol-Lin from oxidation and spares endogenous α -TOH. It seems clear that disappearance of N-TOH (at 5 h) is concomitant to the dramatic increase in the rate of the Chol-Lin oxidation as well as onset of the consumption of endogenous α -TOH. In other words, consumption of α -TOH is not initiated until N-TOH is depleted.

Summary

C(7)-Alkyl-substituted tetrahydro-1,8-naphthyridinols are available by straightforward synthetic approaches, and they show excellent antioxidant profiles in benzene. An α -tocopherol isostere, N-TOH, incorporates into LDL particles and spares consumption of endogenous α -tocopherol under conditions of free radical oxidation. N-TOH has an improved mobility profile in model membrane systems and binds to recombinant human tocopherol transfer protein with better affinity than α -tocopherol itself. *In vivo* studies with N-TOH and some of its derivatives are underway.

Experimental Section

General. Unless noted otherwise, materials were purchased from a commercial supplier and used without further purification. Air- or moisture-sensitive reactions were carried out under an inert gas

(45) Meier, R.; Tomizaki, T.; Schulze-Briese, C.; Baumann, U.; Stocker, A. J. *Mol. Biol.* **2003**, *331*, 725–734.

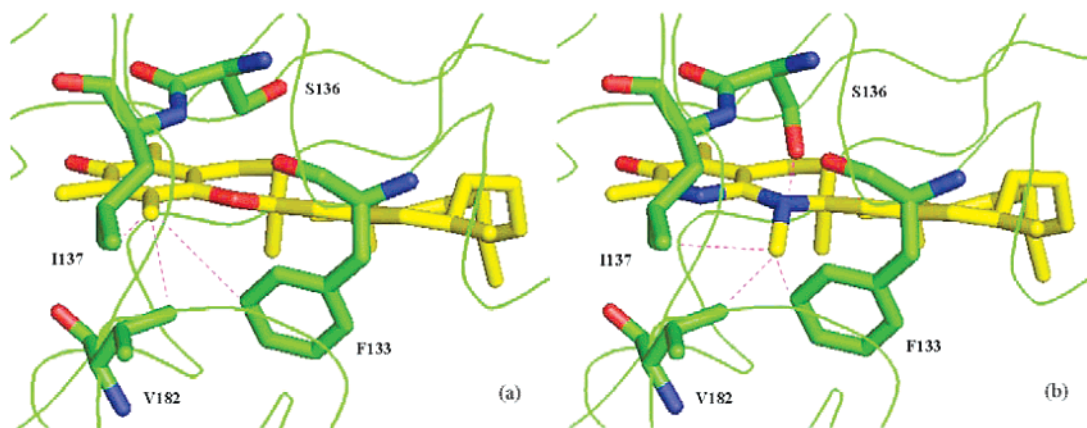


Figure 3. Relevant amino acid side chains of the human tocopherol transfer protein that interact with the positions that differ between α -TOH (a) and N-TOH (b). Reproduced in part from ref 45.

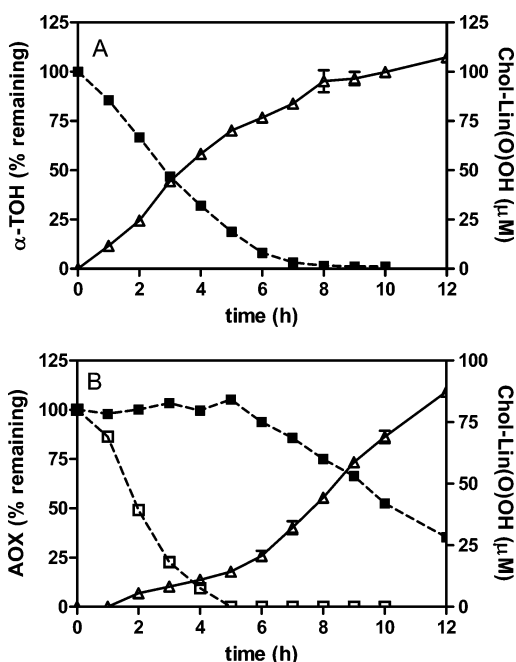


Figure 4. Oxidation of human LDL (0.75 mg/mL protein in PBS buffer) initiated by AIPH (0.5 mM final concentration) at 37 °C. Total cholesteryl linoleate hydroperoxides (Δ) were monitored at 234 nm by HPLC following their reduction to the corresponding alcohols with PPh_3 . Consumption of antioxidant (α -TOH (\blacksquare) and N-TOH (\square)) was monitored by both electrochemical detection and HPLC at 195 and 330 nm: (A) unsupplemented LDL and (B) N-TOH (75 μM)-supplemented LDL.

atmosphere. THF, Et_2O , and CH_2Cl_2 were dried using a solvent purification system from Solvtek. Progress of reaction was monitored by thin-layer chromatography (TLC) using silica gel F_{254} plates. Purification of the products was performed by flash column chromatography using silica gel 60 (230–400 mesh) or a Biotage SP-1 system with indicated solvents. NMR spectra were taken on a 300 or 400 MHz Bruker NMR spectrometer. Chemical shifts (δ) are expressed in ppm using solvent as an internal standard and coupling constant (J) in hertz. HRMS spectra were recorded using the electrospray technique. ESI-HRMS measurements were performed at Ohio State University.

Synthesis. Detailed experimental procedures for the preparation of all new compounds reported herein are presented in the Supporting Information.

Antioxidant Activity in Solution: Determination of k_{inh} . Stock solutions of pentafluorobenzyl (PFB) 13-HOTrE (1.0 M), MeOAMVN (0.05 M), and antioxidant (~ 0.1 M) were prepared in benzene. Oxidation samples were prepared in 1 mL autosampler vials with a

total volume of 100 μL . The solutions were added in the following specific order to prevent premature oxidation of the substrate: antioxidant (0.04–0.08 M), PFB 13-HOTrE (0.1 M), MeOAMVN (2.5 mM). The mixture was then diluted to 100 μL with benzene. The sealed vials were oxidized at 37 °C for 1 h.

After 1 h, the reaction was stopped, and the hydroperoxides were reduced by the addition of 50 μL of 0.1 M butylated hydroxytoluene (BHT) and $\text{P}(\text{OCH}_3)_3$ in hexanes. The samples were then prepared for LC-APCI-MS analysis. The reaction mixtures were loaded onto Varian BondElut, Jr. SPE cartridges that contained 500 mg of silica that had been pre-conditioned with 3 mL of hexanes. After loading of the cartridges, the samples were washed with 5 mL of a hexanes:EtOAc mixture (85:15) to remove excess antioxidant and unoxidized PFB 13-HOTrE. The diols were eluted from the cartridge with 2 mL of EtOAc. The solvent was removed under a stream of N_2 . The diols were redissolved in 250 μL of MeOH:H $_2$ O (80:20) for LC-MS analysis.

For LC-APCI-MS, the diols were separated by RP-HPLC using a Supelco Discovery C-18 column (4.6 mm \times 25 cm) and a MeOH:H $_2$ O solvent gradient (70:30 \rightarrow 90:10) between 5 and 45 min at 1 mL/min. The mass spectrometer was operated with an APCI source in negative-ion mode. The instrumental conditions were as follows: 5 μA corona discharge, 300 °C capillary temperature, 475 °C vaporizer temperature, -20 V capillary voltage, and -35 V tube lens voltage. The diols were then analyzed using selective ion monitoring (SIM) of mass 309 m/z . The peak areas of the 8,13-*c,c,t* diols were then compared to those of the rest of the oxidation products after adjustment of the peak areas by their respective response factors. The response factors convert the individual areas of the mass spectrometry peaks to match those of HPLC peak areas from controlled oxidations using α -TOH as the H-atom donor. A calibration curve from the α -TOH oxidations is then utilized to determine k_{inh} .

Lateral Diffusion Measurements: Determination of D_L . Liposomes were prepared according to the ethanol injection method,⁴⁶ which produces unilamellar liposomes of uniform size and with equally distributed antioxidant and Fluorazophore-L concentration in both lipid leaflets. Fluorazophore-L was synthesized as reported.⁴⁷ 1-Palmitoyl-2-oleoyl-*sn*-glycero-3-phosphocholine was obtained from Sigma (Germany).

The fluorescence decay traces (Figure S1, Supporting Information) were obtained on a time-correlated single-photon-counting fluorometer (FLS920, Edinburgh Instruments Ltd.) equipped with a diode laser (PicoQuant LDH-P-CA375, $\lambda_{\text{exc}} = 373$ nm, $\lambda_{\text{abs}} = 450$ nm, fwhm ca. 50 ps). The temperature was controlled (± 0.1 °C) with a circulating water bath (Julabo F25/HD thermostat). The laser pulse frequency was kept below 2% of the inverse lifetime, while the count rate was set to

(46) Domazou, A. S.; Luisi, P. L. *J. Liposome Res.* **2002**, *12*, 205–220.

(47) Gramlich, G.; Zhang, J.; Winterhalter, M.; Nau, W. M. *Chem. Phys. Lipids* **2001**, *113*, 1–9.

less than 1% of the pulse rate. All experiments were carried out with freshly prepared samples in quartz cuvettes, with a blank measurement (liposomes lacking Fluorazophore-L) at all investigated temperatures to correct for light scattering. Bimolecular quenching rate constants in homogeneous solution were measured as described.^{34,36,37}

Data Analysis. The fluorescence decay traces were treated according to the previously described formalisms.^{34,35} N-TOH showed auto-fluorescence near 450 nm upon 373 nm excitation, which was verified for a freshly HPLC-purified sample. Because this auto-fluorescence ($\tau \approx 7 \pm 0.2$ ns) could not be reliably subtracted or accounted for in the fitting, the fluorescence decay traces were analyzed by tail fitting, i.e., by cutting the initial 100 ns region, thereby accounting for the larger error of the recovered diffusion coefficients.

$$I(t) = I_0 \exp[-(k_0 t + 2.31 D_L N_a [Q_{2D}] t + 7.61 \sqrt{D_L} R N_a [Q_{2D}] \sqrt{t})]$$

Tocopherol Transfer Protein (TTP) Binding Assays. Recombinant human TTP⁴² (0.2 μ M) is incubated with 1.0 μ M NBD-Toc in SET buffer (250 mM sucrose, 1 mM EDTA, 50 mM Tris, pH 7.4) containing 100 μ M Triton X-100 at ~ 20 °C. The fluorescence of NBD-Toc is greatly enhanced on binding to the protein. After the signal has reached equilibrium, small aliquots of competitor (N-TOH or α -TOH) dissolved in EtOH were added, and the signal was monitored until the observed fluorescence decrease came to a steady value. This was accomplished within 15 min and was generally faster for the more water-soluble N-TOH than for α -TOH. The final concentration of EtOH did not exceed 2% (v/v) and was usually less than 1% (v/v). Graphs were made in the Prism software package and are best fit to a two-phase exponential decay, but the reasons for this are not obvious.

Low-Density Lipoprotein Oxidations. Plasma was separated from red blood cells by centrifugation (420 rpm for 10 min at room temperature). N-TOH was dissolved in dimethylsulfoxide (final concentration 75 μ M, final volume <3%), supplemented to the freshly separated plasma, and incubated for 1.5 h at 37 °C. The supplemented

LDL was subsequently isolated from the plasma using sequential density ultracentrifugation (target density = 1.019–1.063 g/mL; this step removes HDL and VLDL). The LDL layer isolated was passed through a PD-10 gel filtration column twice in order to remove aqueous and/or low-molecular-weight compounds such as inorganic salts, aqueous antioxidants, and unincorporated **34**. The supplemented LDL and natural LDL (control; both contain about 0.75 mg of protein/mL) were incubated with AIPH initiator (final concentration 0.5 mM) at 37 °C. Samples were taken every hour for 12 h, including one at 0 h. To a 100 μ L LDL sample were added 30 μ L of BHT (3 mM), 30 μ L of PPh₃ (25 mM), and 1 mL of MeOH. Methyl 13-hydroxy-(9*E*,11*E*)-octadecadienoate and γ -TOH were used as internal standards for the analysis of Chol-Lin and antioxidant (α -TOH and **34**) analysis, respectively. The organic layer was extracted with hexane. Chol-Lin was analyzed by HPLC with 0.4% isopropanol/hexane mobile phase and a Beckman silica column (4.6 mm \times 250 mm, dual column) at 234 nm following their reduction to the corresponding alcohols with PPh₃. Consumption of the antioxidants (α -TOH and **34**) was monitored by both electrochemical detection and HPLC at 195 and 330 nm with 5% H₂O/MeOH mobile phase containing 10 mM LiClO₄ and a Supelco Discovery C₁₈ column (5 μ M, 4.6 mm \times 250 mm).

Acknowledgment. We are grateful for support of this research by NIEHS P01-013125 and the National Science Foundation. D.A.P. acknowledges support of the Natural Sciences and Engineering Research Council of Canada and the Canada Research Chairs program.

Supporting Information Available: Experimental details of syntheses and Figure S1 showing fluorescence decay data. This material is available free of charge via the Internet at <http://pubs.acs.org>.

JA072371M